Computers in Biology and Medicine 104 (2019) 310–318

Contents lists available at ScienceDirect

Computers in Biology and Medicine

journal homepage: www.elsevier.com/locate/compbiomed

# Bimodal classification algorithm for atrial fibrillation detection from m-health ECG recordings☆

Grant H. Kruger[a,b,*,1], Rakesh Latchamsetty[c,1], Nicholas B. Langhals[d], Miki Yokokawa[c], Aman Chugh[c], Fred Morady[c], Hakan Oral[c], Omer Berenfeld[d,e]

[a] Department of Mechanical Engineering, University of Michigan, Ann Arbor, MI, USA
[b] Department of Anesthesiology, University of Michigan, Ann Arbor, MI, USA
[c] Cardiac Arrhythmia Service, University of Michigan, Ann Arbor, MI, USA
[d] Neural Engineering, National Institute of Neurological Disorders and Stroke, National Institute of Health, Bethesda, MD, USA
[e] Center for Arrhythmia Research, University of Michigan, Ann Arbor, MI, USA

ARTICLE INFO

*Keywords:*
Atrial fibrillation
E-health
Frequency domain
Time domain
Rhythm classification

ABSTRACT

*Introduction:* Atrial Fibrillation (AF) is the most common cardiac arrhythmia, presenting a significant independent risk factor for stroke and thromboembolism. With the emergence of m-Health devices, the importance of automatic detection of AF in an off-clinic setting is growing. This study demonstrates the performance of a bimodal classifier for distinguishing AF from sinus rhythm (SR) that could be used for automated detection of AF episodes.

*Methods:* Surface recordings from a hand-held research device and standard electrocardiograms (ECG) were collected and analyzed from 68 subjects. An additional 48 subjects from the MIT-BIH Arrythmia Database were also analyzed. All ECGs were blindly reviewed by physicians independently of the bimodal algorithm analysis. The algorithm selects an artifact-free 6-s ECG segment out of a 20-s long recording and computes a spectral Frequency Dispersion Metric (FDM) and a temporal R-R interval variability (VRR) index.

*Results:* Scatter plots of the VRR and FDM indices revealed two distinct clusters. The bimodal scattering of the indices revealed a linear classification boundary that could be employed to differentiate the SR from AF waveforms. The selected classification boundary was able to correctly differentiate all the subjects from both datasets into either SR or AF groups, except for 3 SR subjects from the MIT-BIH dataset.

*Conclusion:* Our bimodal classification algorithm was demonstrated to successfully acquire, analyze and interpret ECGs for the presence of AF indicating its potential to support m-Health diagnosis, monitoring, and management of therapy in AF patients.

## 1. Introduction

Atrial Fibrillation (AF) is the most common cardiac arrhythmia and results in loss of atrial contractility and an irregular and often rapid ventricular rate [1–3]. In addition to its potential to cause debilitating symptoms and decrease in cardiac contractile function, AF is a major independent risk factor for stroke and thromboembolic events and is associated with increased morbidity and mortality [4,5]. At present there are more than 6 million people affected with AF in the United States. While many younger patients also suffer from AF, the Screening for AF in the Elderly (SAFE) study revealed an increase in prevalence every 10-years after the age of 65 (6% age 65–74, 12% age 75–84, and 16% age 85+) [6].

As opposed to sinus rhythm (SR), when the atria contract in response to a repetitive and synchronized electrical impulse originating from the sinus node, during AF the atria are activated by very rapid and disorganized atrial impulses that may be generated from multiple locations throughout the atria. This causes ineffective atrial contraction and can lead to blood stasis, which can ultimately cause clot formation and stroke. Furthermore, it has been long recognized that patients with AF have a tendency for thrombophilia, independent of the atrial contractile function. The atrio-ventricular node during AF transmits irregular and often very frequent impulses to the ventricles. While the ventricles still contract in response to the normal ventricular impulse

☆ All authors contributed to preparing this manuscript and have approved the content of the final article.

* Corresponding author. 1043C H.H. Dow Building, Department of Mechanical Engineering, University of Michigan, Ann Arbor, MI, 48109, USA.
*E-mail address:* ghkruger@umich.edu (G.H. Kruger).

[1] Drs. Kruger and Latchamsetty equally contributed to the study and are co-first authors.

https://doi.org/10.1016/j.compbiomed.2018.11.016
Received 14 July 2018; Received in revised form 8 November 2018; Accepted 18 November 2018
0010-4825/ 

propagation, they do so in an irregular and often rapid manner that can cause inefficient pumping of blood throughout the body and lead to significant clinical symptoms.

AF can be intermittent (paroxysmal) and terminate spontaneously or persistent, requiring intervention to revert to SR. It may develop in patients with structurally normal hearts as well as in patients with associated comorbidities including structural heart disease. The clinical manifestation of AF is highly variable and a significant proportion of patients with AF may remain asymptomatic but still suffer from an increased stroke risk [3,7]. This makes the accurate and timely diagnosis of AF both clinically important and challenging.

Once the proper diagnosis of AF is made, then anticoagulant drugs can be prescribed based on an individual patient's underlying stroke and bleeding risk. Treatments aimed at reducing or eliminating the burden of AF includes medications, or procedures such as catheter ablation. While the available treatment methods for AF provide various degrees of success, none guarantee complete long-term elimination of AF and it is often difficult to accurately determine the effectiveness of the treatment. Part of the difficulty arises because healthcare professionals will often rely on the patient's subjective assessment of their symptoms to gauge effectiveness, whereas patients, particularly after treatment, may be unaware of their AF. Even after months or years of effective AF suppression, a recurrence will once again carry an elevated stroke risk.

There is thus a critical need for m-health systems to help patients reliably and accurately identify their cardiac rhythm state. However, existing noninvasive personal electrocardiogram (ECG) monitors capable of recording, accurately identifying, and transmitting ECGs are limited and have not been widely endorsed by clinicians [8–12].

This study investigates the preliminary clinical assessment of an automated algorithm for distinguishing AF from SR. An open source personal m-health development platform was used to collect the primary data set, which was further supplemented from the online published MIT-BIH Arrhythmia dataset.

## 2. Methods

The study presented in this manuscript was approved by the Institutional Review Board and was performed in accordance with the ethical standards as laid down in the 1964 Declaration of Helsinki and its later amendments or comparable ethical standards. Informed consent was obtained from all individual participants included in the study.

### 2.1. Datasets

The primary dataset was collected from a series of 20-s long digital ECG recordings, analogous to lead I, utilizing an open-source m-health research device developed at the University of Michigan (UM), shown in Fig. 1. Stainless steel dry electrodes were located on the device and directly connected to a standard fully-differential ECG front-end consisting of an instrumentation pre-amplifier ( × 10 gain), a switched capacitor band-pass filter from 2 to 40 Hz, amplifier ( × 100 gain) and a 16-bit analog-to-digital converter (1.4 kHz sample rate down sampled to 82 Hz). A PIC32MX440 32-bit risk-based MPU running at 80 MHz synchronized the acquisition, digital signal processing, recording, USB/Bluetooth communications and display functions.


**Fig. 1.** The hand-held research device used to collect the ECG signals in the clinical study. The shown trace is a real-time recorded ECG analog to the standard lead I ECG configuration.

This hand-held device was used to record ECGs from 46 patients with AF (23 paroxysmal and 23 persistent) who presented to the Arrhythmia Clinic or Electrophysiology Laboratory at the University of Michigan. The hand-held device was also used in 22 healthy subjects with no AF enrolled to provide baseline SR ECG data, providing a total dataset of 68 subjects with ECG waveforms. The first 20-s long segment of each of the hand-held 68 ECG waveforms was used for the classification analysis. In addition, during the hand-held recordings, a simultaneous reference 5- or 12-lead standard ECG was also acquired utilizing adhesive standard electrodes and analyzed by at least 3 independent, blinded electrophysiologists to confirm either an AF or SR state. In case of a disagreement (< 10% of the tracings), diagnosis was made by a consensus among the 3 senior electrophysiologists.

Further, the MIT-BIH Arrythmia Database consisting of 48 ambulatory lead II and $V_1$ ECG recordings each 30-min long, sampled at 360 Hz with 11-bit resolution was downloaded and included to provide a reference commonly used in prior publications. The recordings were originally made at Beth Israel Hospital Arrhythmia Laboratory between 1975 and 1979 using 9 analog Del Mar Avionics model 445 reel-to-reel Holter recorders and at some time later, digitized and annotated by two cardiologists working independently [13,14]. Detailed descriptions of the database can be obtained from the listed citations or Physionet webpage (www.physionet.org). To incorporate data under similar collection conditions as in our UM-based clinical study, we modified the "rddata.m" MATLAB function (originally contributed to Physionet by R. Tratnig and K. Rheinberger) to search each record for the first occurrence of either a 20-s long SR or AF waveform. For this extraction SR was defined as waveforms with a rhythm annotation "(N" and beats annotated "N", while AF was defined as waveforms with a rhythm annotation "(AFIB". From the original 46 recordings, the resulting dataset consisted of 21 SR and 8 AF 20-s long Lead-II ECG recordings, which were subsequently downsampled to 82 Hz to match the research device. Fig. 2 provides a summary of the research study design.

### 2.2. ECG analysis algorithm

The ECG analysis algorithm presented in this manuscript was implemented in MATLAB (Mathworks, Natick, MA) and consists of 4 phases that will be discussed in the following section: 1) Automatic 6-s waveform selection from a 20-s recording, 2) Time domain analysis, 3) Frequency domain analysis and 4) Classification.

#### 2.2.1. Automatic waveform selection

For wearable or hand-held ECG recorders well-known, frequently encountered, motion artifacts and baseline drift degrade signal quality. Thus, a high pass filter is typically used to remove this drift, however, at times the frequency components in the motion artifacts may propagate into the physiologically relevant portion of the signal. For automated analysis, any artifacts remaining after baseline drift removal should be avoided to minimize erroneous classifications.

At the onset of the analysis procedure the algorithm must select a 6-s long ECG segment that will be used for analysis from the longer 20-s long window. This provides the opportunity for the algorithm to avoid regions where motion artifacts corrupt the signal. To achieve this, we developed an algorithm that computes an artifact severity index (ASI) by computing the ratio of the range of QRS complex peaks to the low frequency drift in the signal. It is important to note that the ASI is designed to exclude segments with drift and motion artifacts, and not rhythms other than AF or SR, such as premature ventricular contractions or bigeminy.

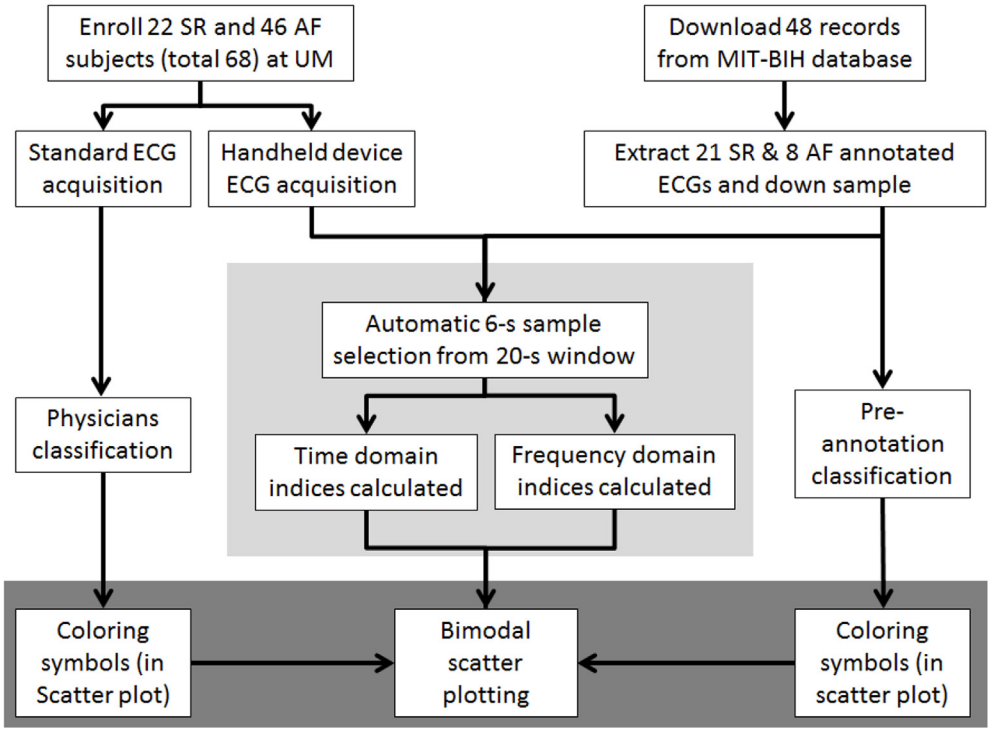


**Fig. 2.** Flow chart of study to analyze the detection of SR and AF from waveforms obtained from enrolled UM subjects using a standard clinical ECG and research system (left arm), and annotated MIT-BIH data downloaded from Physionet (right arm). The light gray rectangle indicates the algorithm this manuscript reports on. Dark gray rectangle indicates the rhythm detection analysis.

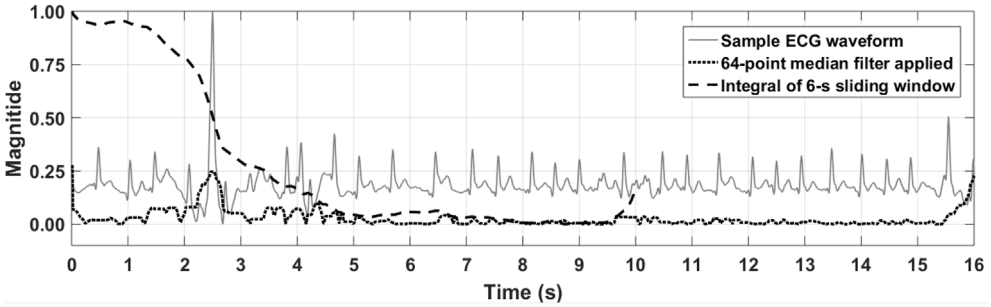


**Fig. 3.** Example of 20-s long waveform analysis for a sub-selection of the 6-s segment. The artifact severity index (ASI; dashed line) shows minimal values between about 5- and 15-s from which the 6-s long segment could be selected.

The ASI metric is calculated from the range in magnitude of the QRS complex peaks as estimated using a 2-s sliding window that records the maximum signal magnitude across the 20-s long waveforms. The ratio between the global maximum to median of the signal is then computed. Signals with large spikes will exhibit higher values, compared to signals with more regular QRS peak morphology. Thereafter, a 64-point (0.8 s) median filter is applied to the original 20-s waveform to remove peaks and reveal the underlying baseline drift. The resulting signal is zero-centered, absolute value taken and scaled by the peak variability metric computed in the previous step. An example of the result of this processing step is shown in Fig. 3, as the dotted line. Peaks can be seen around the areas of motion artifact between 1 and 5 s in the graph. The optimal position for the 6-s sub-waveform is computed by taking the minimum of the integral computed over a 6-s window for each starting location within the 20-s window. The dashed line in the graph indicates that a 6-s window starting at < 5s within the 20-s window may be corrupted by artifact. The first and last 2-s of all 20-s long signals are discarded due to the high prevalence of artifacts in these regions.

### 2.2.2. Time-domain algorithm

An R-wave detection algorithm was utilized for heart rate variability analysis. Automatic classification of cardiac rhythm using heart rate variability analysis has been widely utilized as a diagnostic tool for rhythm disorders [15,16]. The algorithm we implemented performs the R-wave detection by applying a band-pass Finite Impulse Response (FIR) zero-phase 1st order Butterworth filter with a 15–20 Hz pass band (10 and 25 Hz stop band corner frequencies), 3 dB pass-band ripple and 10 dB stop-band attenuation to the 6-s long selected waveform. The filtering removed all low and high frequency components of the signal and provided a rounded waveform in the vicinity of the QRS complex. Thereafter, a threshold was defined at 40% of the maximum magnitude over the filtered 6-s waveform and used with the "findpeaks" MATLAB function (with 366 ms minimum peak distance) to locate each QRS complex. Around each peak position estimate, the local maximum over a ± 60 ms windows was obtained using the original unfiltered 6-s waveform to reveal the true peak position of the QRS complex.

From the peak position data the standard deviation of the R-wave intervals were calculated and normalized to the mean R-wave interval, to obtain the dimensionless measure of variance of the R-waves intervals (VRR score).

### 2.2.3. Frequency-domain algorithm

We hypothesized that the ECGs exhibiting SR signals would be composed of periodic, narrow-frequency bands. However, we expected the frequency spectrum of AF waveforms to be more dispersed. To evaluate this hypothesis we calculated the power spectra of the

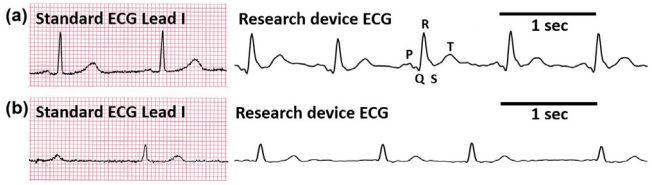


**Fig. 4.** Comparison between ECGs collected during the clinical study using the research device (analogous to lead I) and the corresponding standard clinical ECG, showing comparisons between a SR patient (a) and AF patient (b). A standard ECG signal is shown for reference.

analyzed signals and quantified their frequency dispersion as follows: The algorithm applied a zero-phase 10th order Butterworth band-pass FIR filter with 2.5–8.0 Hz pass-band filter (2.0 and 10 Hz stop-band corner frequencies, 3 dB pass-band ripple and 30 dB stop-band attenuation) to the 6-s ECG signal to select the frequency range of interest [17,18]. Thereafter, the Fast Fourier Transform (FFT) was computed on the output of the filter. The 6-s signal sampled at 82 Hz for 492 samples was zero-padded equally on either side of the samples to form the 1024 data point series for the FFT. The FFT bin with the peak magnitude was then identified, and this magnitude was divided by the sum of the magnitudes across all bins to obtain the dimensionless frequency dispersion metric (FDM).

## 3. Results

Fig. 4 provides a comparison between an ECG recorded from two enrolled subjects, one with AF and one in SR, using the UM research device and standard clinical ECG machine. The time-domain ECG acquired through the research device closely matched the corresponding simultaneous standard lead I ECG signal.

Fig. 5 shows the time- and frequency-domain analyses of the ECGs acquired from the 2 patients shown in Fig. 4. Fig. 5(a) shows that there is greater variability in the R-R intervals for the patient with AF compared to the subject in SR, resulting in a VRR score of 0.16 and 0.01, respectively. From Fig. 5(b) it can be seen that the frequency domain prior to band-pass filtering is characterized by well-organized periodic frequency peaks during SR, whereas during AF, the energy is more dispersed at low power peaks as can be seen in Fig. 5(b). The FDM score is therefore consequently higher in the AF case compared to the SR case (11.30 vs. 8.93).

A scatter plot of the FDM and VRR scores for all subjects enrolled in the study and those from the MIT-BIH database demonstrated two clearly distinct clusters for the unclassified data as shown in Fig. 6. Each point indicates the score obtained from a single unclassified subject's 6-s ECG sample. The color of each data point represents the physician's classification of the waveform, with hot colors indicating AF (red = UM AF subject, yellow = MIT-BIH AF subject) and cool colors indicating SR (blue = UM SR subject, green = MIT-BIH SR subject).

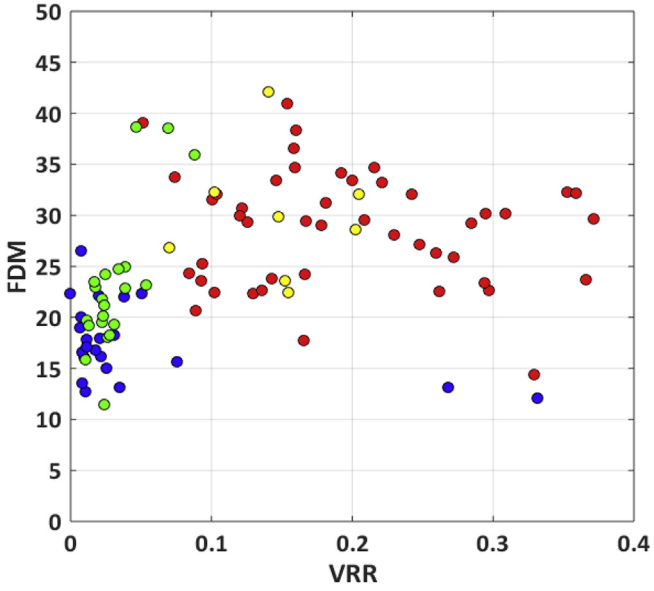


**Fig. 6.** Scatterplot of FDM vs. VRR indices for each of the 68 UM research device acquired ECGs and 29 analyzed MIT-BIH waveforms. Colors indicate: blue/red = UM SR/AF subject, green/yellow = MIT-BIH SR/AF subjects.

On combinations of the VRR, FDM and heart rate results from both datasets we performed the Lilliefors test for normality at both the 5% and 10% significance levels. The heart rate data for both datasets and their combination was found to be normally distributed and the Student's t-test was used to evaluate significance between the SR and AF sub-sets. A summary of the statistical analysis for the heart rate data is provided in Table 1. The results for normal distribution testing for the VRR and FDM metrics remained consistent between significance levels but did not remain consistent between database sub-sets. In cases where a non-normal distribution was found the Lillifors test for an exponential distribution was also performed, however, none were found. The Wilcoxon Signed Rank Test was therefore used to evaluate dependence between the VRR and FDM metrics for the SR and AF subsets. A summary of this analysis is provided in Table 2, which provides the minimum, 1st Quartile, 2nd Quartile (median), 3rd Quartile, maximum, outcome of Lillifors and Wilcoxon tests for the UM, MIT-BIH datasets and their combination. Thereafter, Spearman's Rank Correlation

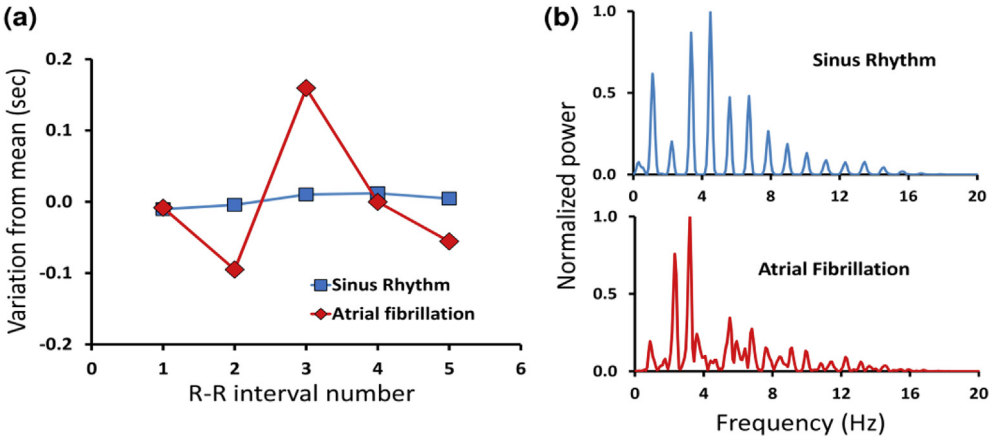


**Fig. 5.** Signal analyses from sample patients in SR (blue) and AF (red) showing (a) typical R-R variability time domain analysis and (b) power spectra for frequency domain rhythm analyses.

**Table 1**
Summary of heart beat rate statistical analysis for various datasets.

| Dataset | Sub-set | Mean + - std. | Significance (*t*-test) |
|---|---|---|---|
| UM | SR | 79 ± 14 bpm | p = 0.22 |
| | AF | 83 ± 16 bpm | |
| MIT-BIH | SR | 73 ± 16 bpm | p = 0.06 |
| | AF | 86 ± 14 bpm | |
| Combined | SR | 76 ± 15 bpm | p = 0.01 |
| | AF | 84 ± 16 bpm | |

Coefficient was computed between the VRR and FDM metrics for each dataset, with a summary of this analysis provided in Table 3. Interestingly, the FDM –VRR correlation for both the SR and AF subjects were negative in almost all cases, suggesting that potentially the FDM and VRR each provide separate and unique information contributing to the separation of the two rhythm groups [19].

### 3.1. Classification

In order to utilize these results to develop a system capable of discriminating between SR and AF a classification method needed to be employed. The clustering present in the bimodal scatter plot of the FDM and VRR metrics shown in Fig. 6 suggested that a hyperbolic function may be able to entirely separate the SR and AF cases. Transforming the VRR axis by taking $VRR^{-1}$, enabled a linear boundary to be used to separate the groups, as shown in Fig. 7. The statistical analysis summary for the transformed $VRR^{-1}$ metric is provided in Table 4, with the Spearman correlation coefficients provided in Table 5. As for the FDM – VRR correlation, the FDM – $VRR^{-1}$ correlation for both the SR and AF patients was also found to be negative.

We described the linear separation boundary using a polar co-ordinate system that specified its pole (origin of the co-ordinate system) along the y-axis and a polar angle. To determine the coefficients of the linear separation boundary we performed an iterative search of candidate pole locations and polar angles. For each pole location candidate, the separation angle between the narrowest SR and AF data points of the UM database (blue and red points in Fig. 7) was computed, and then full histograms of angles of the two rhythms were created for evaluation of the level of separation. As shown in Fig. 8(a) the pole located at FDM = 10.6 (arrow) provided the maximum separation (difference) angle between the minimum AF data point and maximum SR data point. The histograms of the polar angles with the optimal pole for separation between each SR and AF data point at FDM = 10.6 is shown in Fig. 8(b). A gap can be seen between the histograms, indicating complete separation between the groups. When the classification of the SR and AF sets are based on the angle at the center of the gap between the SR and AF histograms, with polar angle of 0.7 radians (arrow), the linear boundary follows the FDM = 10.6 + 3.77 × $VRR^{-1}$ formula, which is superimposed on the scatterplot of Fig. 7 (dotted line). This direct linear separation boundary classifies correctly 99.5% of SR cases and 96.6% of AF cases from both the UM and the MIT-BIH datasets.

The histograms in Fig. 8(b) are based on the study SR and AF dataset. To extrapolate our study dataset to the whole population the histograms were modeled further by probability distribution functions selected based on best-fitting (black traces superimposed on the histograms). It was found that a Beta distribution model provided the best fit

**Table 3**
Summary of Spearman correlation analysis between FDM and VRR.

| Dataset - | | n | Spearman ρ | p |
|---|---|---|---|---|
| UM | SR | 22 | −0.39 | 0.08 |
| | AF | 46 | −0.06 | 0.68 |
| MIT-BIH | SR | 21 | **0.59** | **0.01** |
| | AF | 8 | −0.21 | 0.62 |
| Combined | SR | 43 | 0.17 | 0.28 |
| | AF | 54 | −0.04 | 0.78 |

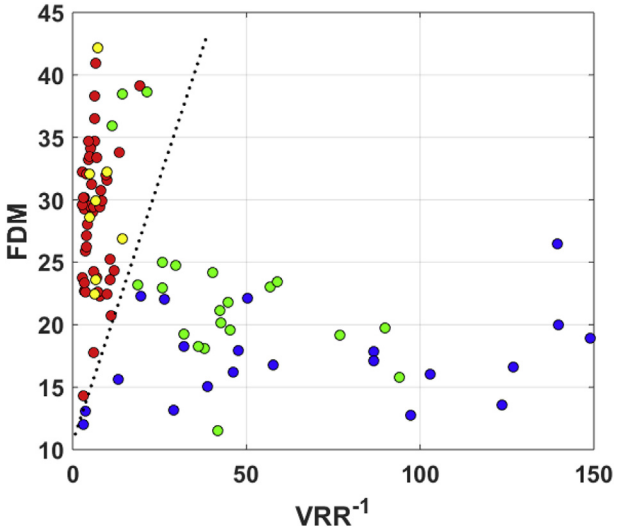


**Fig. 7.** Scatterplot of FDM and VRR metrics for each subject with $VRR^{-1}$ transformed axis enabling a linear classification boundary (dotted line). The method for calculating the optimal linear separation boundary (dotted line) is provided in Fig. 8. Colors indicate: blue/red = UM SR/AF subject, green/yellow = MIT-BIH SR/AF subjects.

**Table 2**
Statistical analysis results for FDM and VRR metrics computed from the databases utilized in this study.

| Var. | Dataset | | n | Min. | 1st Q | Med. | 3nd Q | Max. | Nml. | Significance |
|---|---|---|---|---|---|---|---|---|---|---|
| VRR | UM | SR | 22 | 0.00 | 0.01 | 0.02 | 0.03 | 0.33 | No | p < 0.001 |
| | | AF | 46 | 0.05 | 0.13 | 0.17 | 0.26 | 0.37 | Yes | |
| | MIT-BIH | SR | 21 | 0.01 | 0.02 | 0.02 | 0.04 | 0.09 | No | p < 0.001 |
| | | AF | 8 | 0.07 | 0.12 | 0.15 | 0.18 | 0.20 | Yes | |
| | Combined | SR | 43 | 0.00 | 0.01 | 0.02 | 0.04 | 0.33 | No | p < 0.001 |
| | | AF | 54 | 0.05 | 0.13 | 0.17 | 0.25 | 0.37 | No | |
| FDM | UM | SR | 22 | 12.03 | 15.05 | 16.94 | 19.99 | 26.48 | Yes | p < 0.001 |
| | | AF | 46 | 14.33 | 23.77 | 29.49 | 32.25 | 40.96 | Yes | |
| | MIT-BIH | SR | 21 | 11.50 | 19.26 | 21.81 | 24.34 | 38.62 | No | p = 0.01 |
| | | AF | 8 | 22.46 | 25.21 | 29.26 | 32.17 | 42.15 | Yes | |
| | Combined | SR | 43 | 11.50 | 16.30 | 19.28 | 22.76 | 38.62 | No | p < 0.001 |
| | | AF | 54 | 14.33 | 23.77 | 29.49 | 32.24 | 42.15 | Yes | |

Key: Var. = variable; n = number of observations; Min. = Minimum; Q = Quartile; Med. = Median; Max. = Maximum; Nml. = Normal Distribution (rejection of Lillie Test null hypothesis at 5% significance level); Sig. = Significance of group separation.

**Table 4**
Statistical analysis results for $VRR^{-1}$ metric computed from the databases.

| Var. | Dataset | | N | Min. | 1st Q | Med. | 2nd Q | Max. | Nml. | Sig. |
|---|---|---|---|---|---|---|---|---|---|---|
| $VRR^{-1}$ | UM | SR | 22 | 3.02 | 28.96 | 53.94 | 102.77 | 148.98 | Yes | $p < 0.001$ |
| | | AF | 46 | 2.69 | 3.82 | 5.80 | 7.95 | 19.41 | No | |
| | MIT-BIH | SR | 21 | 11.31 | 25.89 | 40.22 | 48.17 | 94.00 | No | $p < 0.001$ |
| | | AF | 8 | 4.89 | 5.71 | 6.67 | 8.44 | 14.22 | No | |
| | Combined | SR | 43 | 2.69 | 4.04 | 6.03 | 7.95 | 19.41 | No | $p < 0.001$ |
| | | AF | 54 | 3.02 | 27.05 | 42.72 | 86.63 | 148.98 | No | |

Key: n = number of observations; Min. = Minimum; Q = Quartile; Med. = Median; Max. = Maximum; Nml. = Normal Distribution (rejection of Lillie Test null hypothesis at 5% significance level); Sig. = Significance of group separation.

**Table 5**
Summary of Spearman correlation analysis between FDM and $VRR^{-1}$.

| Dataset - | | N | Spearman ρ | p |
|---|---|---|---|---|
| UM | SR | 22 | 0.33 | 0.13 |
| | AF | 46 | 0.06 | 0.68 |
| MIT-BIH | SR | 21 | **−0.59** | **0.01** |
| | AF | 8 | 0.21 | 0.62 |
| Combined | SR | 43 | −0.18 | 0.25 |
| | AF | 54 | 0.04 | 0.78 |

**Table 6**
Performance summary for optimal classification boundary.

| Dataset | TP | FP | TN | FN | PPV (%) | Sensitivity (%) | Specificity (%) |
|---|---|---|---|---|---|---|---|
| UM | 46 | 0 | 22 | 0 | 100 | 100 | 100 |
| MIT-BIH | 8 | 3 | 18 | 0 | 73 | 100 | 86 |
| Combined | 54 | 3 | 40 | 0 | 95 | 100 | 93 |

to the SR histogram (blue, $p < 0.005$, $R^2 = 0.81$), while a Log-Normal distribution model provided the best fit to the AF histogram (red, $p < 0.005$, $R^2 = 0.76$). Based on the general population modeled by the Beta and Log-Normal distributions it was determined that the best separation for the population at large would be at a polar angle of 0.62 radians, which yields a correct classification of 98.4% of SR cases and 97.5% of AF cases, close to what is obtained by the direct study data classification in Fig. 7.

As is evident from Fig. 7, using the direct classification boundary resulted in a perfect separation of the data points representing the 68 subjects enrolled at UM. However, 3 SR cases from the 29 cases included from MIT-BIH dataset were misclassified as AF, resulting in false positives reducing the specificity to 19/21 = 90% and positive predictive value (PPV) to 8/(8 + 3) = 73% for the MIT-BIH dataset. Overall, this reduced the specificity to 40/43 = 93% and PPV to 54/57 = 95% when considering the combined dataset. A summary of these results are provided in Table 6.

Upon inspection of the raw MIT-BIH data, it was suggested that the reason for the 3 false positive AF detections in the MIT-BIH dataset is the result of the different acquisition method relative to our hand-held recording device. First, in the lead II configuration of the MIT-BIH dataset, the ratio of the QRS to the P complexes amplitude is different than in the lead I configuration of the hand-held device, which may have affected the FDM calculation. Second, it may have happened that, as in many typical ECG acquisition systems, the MIT-BIH signals were high-band pass filtered to enhance the deflections of the main complexes, while this was not performed in the hand-held device recordings. The 2.5–8 Hz band-pass filter employed may not adequately attenuate this larger deflection present in the Lead II recordings of the MIT-BIH dataset. The effect of these factors on the FDM and VRR metrics could be the reason for the miss-classification of the 3 MIT-BIH cases and will require further consideration. These factors will be investigated in greater depth in subsequent studies incorporating larger numbers of Lead II recordings.

To further evaluate the robustness of the classification results shown in Figs. 7 and 8, we utilized a 10-fold cross validation technique. Accordingly, for each fold 2/3 of the UM and MIT-BIH combined dataset was randomly sampled and utilized as training data to build the SR and AF histogram models, as shown in Fig. 8(b). The remaining 1/3 of the data was utilized as test data to evaluate the performance of the classifier. Variations in the best-fit of the SR and AF probability density functions resulted in fluctuations of their intercept point on the x-axis and hence the corresponding ideal polar angle for the linear classification boundary. Considering all 10 iterations, the y-intercept of FDM was 10.65 ± 0.36 (mean ± standard deviation), with a polar angle of 0.59 ± 0.04 radians (compare with Fig. 7). These results provide a projected classification accuracy of 97.0 ± 2.8% for SR cases and 97.4 ± 0.7% for AF cases. Across the 10 folds, on 3 occasions 1 MIT-BIH subject from the test dataset was misclassified as a false positive and on another 3 occasions the same MIT-BIH subject was misclassified along with 1 UM subject from the test dataset (the misclassified SR datapoints were located closest to linear separation boundary shown in

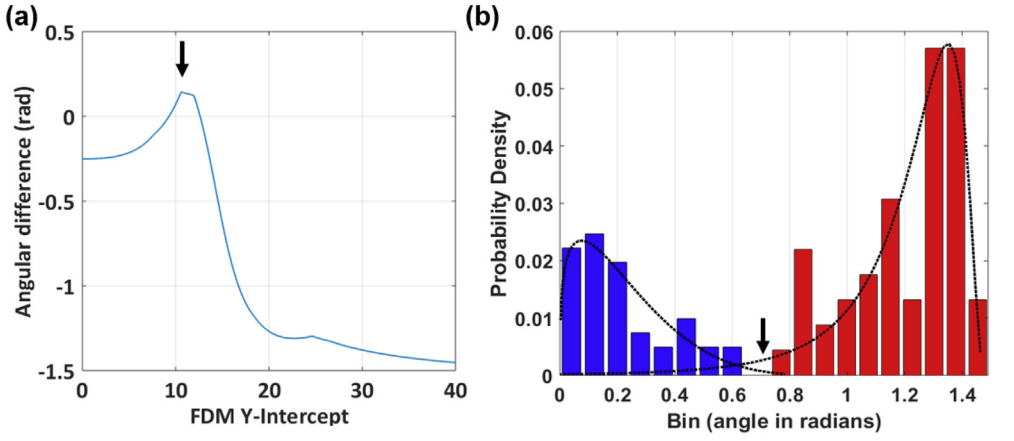


**Fig. 8.** Determination of the linear classification boundary coefficients for Fig. 7 a) Angular difference between most adjacent physician-classified SR and AF data points versus candidate pole position along the vertical axis of Fig. 7. The maximal difference is obtained at FDM = 10.6 (arrow). b) Probability distribution histograms for physician-classified SR (blue) and AF (red) datasets for polar angles around the pole origin at FDM = 10.6. The histograms are separated at 0.7 radians (arrow). Best-fitted probability distribution functions are superimposed on histograms for estimation of the separation in the general population.

Fig. 7). However, when utilizing the mean y-intercept and polar angle for the linear classification boundary over all 10 folds, the same performance was obtained as when a polar angle of 0.62 or 0.70 radians was used for the entire dataset analysis.

## 4. Discussion

This is an initial clinical evaluation of an automated bimodal algorithm for AF detection for m-health rhythm monitoring. The analytic algorithm integrates time- and frequency-domain signal processing and calculation of two physiological metrics, which allows a simple linear function to be used to assign membership of new data points to either an AF or SR state for rhythm classification. The system provides a convenient method to analyze short single-lead ECG samples for the rapid detection of AF with excellent diagnostic accuracy.

### 4.1. AF detection

The detection of AF based on ECG signals can be challenging for automated algorithms [20–23]. Traditional algorithms to detect the presence of AF from intracardiac or surface ECGs typically analyze the duration of the intervals between sequential atrial activations [24] and irregular response of the ventricle to AF [25–27] and rely heavily on the statistical analysis of the R-wave timing and RR intervals. For surface ECG recordings, this approach can be suboptimal due to several factors including inaccurate detection of R waves [28] and requiring relatively long recordings of at least 30-s [29] to collect sufficient data.

However, there is no clear physiological rationale for utilizing a minimum ECG recording of 30-s length for AF detection. In fact, a recent clinical study found that patients with atrial arrhythmias lasting 5 beats to 30-s were at significantly higher risk to develop clinical AF and stroke compared with those with no documented short atrial arrhythmias [30]. These findings raise important questions about the meaning of very brief episodes of atrial arrhythmia and their relationship to future AF and stroke events [31,32]. We thus believe tools should be developed that will enable the exploration of short AF episodes to better understand the etiology of AF initiation as well as the predictive value of short episodes.

The algorithm proposed by this manuscript has the ability to detect short durations of AF using a bimodal analysis of physiological time and frequency components. Since the linear classification boundary, shown in Fig. 7, is not perpendicular to either X- or Y-axes, it is suggested that the detection of AF benefits from the bimodal time-frequency classification approach we employ. The frequency-domain analysis captures information from both the atrial (p-wave) and ventricular (QRS-complex) components of the ECG waveform instead of just ventricular activations timing when analyzing merely the R-R intervals. It has been established experimentally that during AF, cardiac electrical activity undergoes a dramatic shift that increases dispersion in atrial frequency content and irregularity [33–36]. It has also been demonstrated clinically that the intra-atrial frequency content during AF [37] is reflected well in signals on the body surface [18,38]. Consistent with these studies, the ECG signals in this study exhibited higher frequency dispersion in AF than in SR within the frequency range of 2 and 20 Hz, as shown in Fig. 5(b). Using frequency-domain analysis, the entire signal is considered instead of only a few discrete time markers captured from each cardiac cycle. Ideally, the increased use of information by the frequency-domain analysis means that shorter waveform segments could be used to detect AF, which may be important when asking what is the minimum length for an AF episode before an intervention is warranted [30,31]. Furthermore, the ability to perform accurate classification using a minimum recording length is beneficial for embedded monitoring devices operating on limited storage and power, such as implantable or injectable devices [39]. Furthermore, the rapid detection of AF could also help prevent inappropriate shocks from ICDs without putting the patient at risk for delayed appropriate therapies for ventricular arrhythmias.

It should also be recognized that many other groups have also developed algorithms and devices for AF detection; however, publications on commercial devices such as the MyDiagnostick, AFibAlert, LINQ or AliveCor, limit detailed discussion on their algorithms and focus only on the clinical results [23,40,41]. Furthermore, many research groups focusing on algorithm development tend to only test their algorithm using pre-recorded data available online from databases such as Physionet (MIT-BIH AF, MIT-BIH Arrhythmia, and MIT-BIH Normal SR with 25, 48 and 18 patients respectively) [42–44]. However, much of these data seem to have been collected on dated acquisition systems (i.e. magnetic tape) with unknown preprocessing features and contain artifacts from known (i.e. mechanical components) and unknown (i.e. motion artifact) sources. Even though these databases provide a great resource, the lack of direct high-resolution digital acquisition and storage in a controlled environment as well as small patient sample size, limit the evaluation of algorithms based on these data.

### 4.2. Clinical utility

The actual clinical benefits or harm by classifying SR and AF rhythms, even if accurate, require randomized clinical trials. Notwithstanding, we speculate that the general use of personal ECG monitors with the ability to immediately and automatically classify a patient's rhythm status may have the following implications: 1) It may facilitate the timely confirmation of AF to support the initiation and management of an appropriate therapy. However, based on current knowledge there is ongoing debate as to whether AF screening using handheld ECG devices will be effective and sustainable [45–48]; 2) AF can recur long after a successful therapy, and an accurate personal monitor may empowers the patient to self-monitor their response to the intervention [49–51]; 3) The need to manually and individually review each ECG with personal ECG systems has been a major limiting factor for wide adoption of existing monitoring systems among health care providers. Should very high diagnostic accuracy be achieved, the algorithm could also be used to automatically analyze large volumes of data and may facilitate the wider adoption of mobile rhythm monitoring by both patients and providers; 4) The AF detection algorithm discussed in this article could also be incorporated into standard clinical bed-side ECG devices to improve their diagnostic accuracy in detecting AF and reduce alert fatigue when used in intensive care and telemetry units [52,53]; and 5) The system may be suitable to be incorporated into implantable cardioverter defibrillators to prevent inappropriate shocks due to AF with rapid ventricular rates.

It should be noted that at the current time, even if the diagnosis made by an algorithm using 6-s or even 20-s segments of data is accurate, it does not necessarily confer any specific prognostic action since current guidelines require longer and repeated measurements before these data impact patient care. However, AF is often progressive, with short episodes at initial stages of the arrhythmia, and the detection of those short episodes of AF may lead to heightened awareness and more robust monitoring before a patient presents with a major complication, such as stroke [31,54,55].

### 4.3. Limitations

Although we have demonstrated a separation of the data in AF and SR member clusters based on estimates of the SR and AF analytical data distributions, a larger sample of the population would enable a more robust measure of the true probability distributions for each group. As the detection of brief episodes of AF is challenging at this time, additional patient data are required to fully validate the algorithm presented in this manuscript. As we move forward and collect additional data, our classification approach inherently possesses the ability to improve, as new patient data are incorporated into the database and probability distribution functions.

Another limitation of this study is that our AF rhythm classification considered all atrial tachyarrhythmias alike, including atrial flutter. However, atrial flutter has the same clinical implications as AF and therefore our classification is to be considered a helpful incremental utility. Larger follow-up studies to fully evaluate the robustness of our algorithm against other arrhythmias, including sinus arrhythmia and premature beats are planned. The performance of the algorithm with older patients and variable signal quality, when used in unsupervised real-world settings, also remains to be studied.

## 5. Conclusion

We have demonstrated in a preliminary clinical investigation of 6-s long signals collected using a handheld m-health digital ECG recorder, the new algorithm is capable of detecting AF with high accuracy using the combination of time- and frequency-domain physiological metrics. Accurate performance of this and similar algorithms operating on personal m-health devices have the potential to help both physicians and patients for the early detection of AF.

## Conflicts of interest

None Declared.

## Acknowledgements

*Funding*

The study was supported in part by grants from the Coulter Translational Research Partnership program from the Department of Biomedical Engineering at the University of Michigan.

*Ethical approval*

"All procedures performed in studies involving human participants were in accordance with the ethical standards of the institutional and/or national research committee and with the 1964 Helsinki declaration and its later amendments or comparable ethical standards."

This article was prepared while Dr. Langhals was employed at The National Institute of Neurological Disorders and Stroke. The opinions expressed in this article are the author's own and do not reflect the view of the National Institutes of Health, the Department of Health and Human Services, or the United States government.

## References

[1] Y. Miyasaka, M.E. Barnes, K.R. Bailey, S.S. Cha, B.J. Gersh, J.B. Seward, T.S. Tsang, Mortality trends in patients diagnosed with first atrial fibrillation: a 21-year community-based study, J. Am. Coll. Cardiol. 49 (2007) 986–992.

[2] C. Gutierrez, D.G. Blanchard, Atrial fibrillation: diagnosis and treatment, Am. Fam. Physician 83 (2011) 61–68.

[3] M.A. Crandall, D.J. Bradley, D.L. Packer, S.J. Asirvatham, Contemporary management of atrial fibrillation: update on anticoagulation and invasive management strategies, Mayo Clin. Proc. 84 (2009) 643–662.

[4] P.A. Wolf, R.D. Abbott, W.B. Kannel, Atrial fibrillation as an independent risk factor for stroke: the Framingham Study, Stroke; A J. Cerebral Circul. 22 (1991) 983–988.

[5] F.D. Hobbs, A.K. Roalfe, G.Y. Lip, K. Fletcher, D.A. Fitzmaurice, J. Mant, Performance of stroke risk scores in older people with atrial fibrillation not taking warfarin: comparative cohort study from BAFTA trial, BMJ 342 (2011) d3653.

[6] F.D. Hobbs, D.A. Fitzmaurice, J. Mant, E. Murray, S. Jowett, S. Bryan, J. Raftery, M. Davies, G. Lip, A randomised controlled trial and cost-effectiveness study of systematic screening (targeted and total population screening) versus routine practice for the detection of atrial fibrillation in people aged 65 and over. The SAFE study, Health Technol. Assess. 9 (2005) 1–74 iii-iv, ix-x.

[7] J.S. Healey, S.J. Connolly, M.R. Gold, C.W. Israel, I.C. Van Gelder, A. Capucci, C.P. Lau, E. Fain, S. Yang, C. Bailleul, C.A. Morillo, M. Carlson, E. Themeles, E.S. Kaufman, S.H. Hohnloser, A. Investigators, Subclinical atrial fibrillation and the risk of stroke, N. Engl. J. Med. 366 (2012) 120–129.

[8] J.K. Lau, N. Lowres, L. Neubeck, D.B. Brieger, R.W. Sy, C.D. Galloway, D.E. Albert, S.B. Freedman, iPhone ECG application for community screening to detect silent atrial fibrillation: a novel technology to prevent stroke, Int. J. Cardiol. 165 (2013) 193–194.

[9] L. Desteghe, Z. Raymaekers, M. Lutin, J. Vijgen, D. Dilling-Boer, P. Koopman, J. Schurmans, P. Vanduynhoven, P. Dendale, H. Heidbuchel, Performance of handheld electrocardiogram devices to detect atrial fibrillation in a cardiology and geriatric ward setting, Europace 19 (2017) 29–39.

[10] J.P.J. Halcox, K. Wareham, A. Cardew, M. Gilmore, J.P. Barry, C. Phillips, M.B. Gravenor, Assessment of remote heart rhythm sampling using the AliveCor heart monitor to screen for atrial fibrillation: the REHEARSE-AF study, Circulation 136 (2017).

[11] A.N. Koshy, J.K. Sajeev, A.W. Teh, Letter by Koshy et al Regarding Article, "Assessment of Remote Heart Rhythm Sampling Using the AliveCor Heart Monitor to Screen for Atrial Fibrillation: the REHEARSE-AF Study", Circulation 137 (2018) 2191–2192.

[12] J.P.J. Halcox, K. Wareham, Response by Halcox and Wareham to letter regarding article, "assessment of remote heart rhythm sampling using the AliveCor heart monitor to screen for atrial fibrillation: the REHEARSE-AF study", Circulation 137 (2018) 2193–2194.

[13] A.L. Goldberger, L.A.N. Amaral, L. Glass, J.M. Hausdorff, P.C. Ivanov, R.G. Mark, J.E. Mietus, G.B. Moody, C.-K. Peng, H.E. Stanley, PhysioBank, PhysioToolkit, and PhysioNet, Components of a New Research Resource for Complex Physiologic Signals vol. 101, (2000), pp. e215–e220.

[14] G.B. Moody, R.G. Mark, The impact of the MIT-BIH arrhythmia database, IEEE Eng. Med. Biol. Mag. 20 (2001) 45–50.

[15] R.J. Oweis, B.O. Al-Tabbaa, QRS detection and heart rate variability analysis: a survey, Biomed. Sci. Eng. 2 (2014) 13–34.

[16] D. Duverney, J.-M. Gaspoz, V. Pichot, F. Roche, R. Brion, A. Antoniadis, J.-C. BarthÉLÉMy, High accuracy of automatic detection of atrial fibrillation using wavelet Transform of heart rate intervals, Pacing Clin. Electrophysiol. 25 (2002) 457–462.

[17] F. Atienza, J. Almendral, J. Jalife, S. Zlochiver, R. Ploutz-Snyder, E.G. Torrecilla, A. Arenal, J. Kalifa, F. Fernandez-Aviles, O. Berenfeld, Real-time dominant frequency mapping and ablation of dominant frequency sites in atrial fibrillation with left-to-right frequency gradients predicts long-term maintenance of sinus rhythm, Heart Rhythm 6 (2009) 33–40.

[18] M.S. Guillem, A.M. Climent, J. Millet, A. Arenal, F. Fernandez-Aviles, J. Jalife, F. Atienza, O. Berenfeld, Noninvasive localization of maximal frequency sites of atrial fibrillation by body surface potential mapping, Circulation. Arrhythmia and Electrophysiol. 6 (2013) 294–301.

[19] O.V. Demler, M.J. Pencina, R.B. D'Agostino, Impact of correlation on predictive ability of biomarkers, Stat. Med. 32 (2013) 4196–4210.

[20] J.M. Davidenko, L.S. Snyder, Causes of errors in the electrocardiographic diagnosis of atrial fibrillation by physicians, J. Electrocardiol. 40 (2007) 450–456.

[21] R.C. Seet, P.A. Friedman, A.A. Rabinstein, Prolonged rhythm monitoring for the detection of occult paroxysmal atrial fibrillation in ischemic stroke of unknown cause, Circulation 124 (2011) 477–486.

[22] S.J. Podd, C. Sugihara, S.S. Furniss, N. Sulke, Are implantable cardiac monitors the 'gold standard' for atrial fibrillation detection? A prospective randomized trial comparing atrial fibrillation monitoring using implantable cardiac monitors and DDDRP permanent pacemakers in post atrial fibrillation ablation patients, Europace 18 (2015).

[23] P. Sanders, H. Pürerfellner, E. Pokushalov, S. Sarkar, M. Di Bacco, B. Maus, L.R. Dekker, R.L.U. Investigators, Performance of a new atrial fibrillation detection algorithm in a miniaturized insertable cardiac monitor: results from the Reveal LINQ Usability Study, Heart Rhythm 13 (2016).

[24] X. Du, N. Rao, M. Qian, D. Liu, J. Li, W. Feng, L. Yin, X. Chen, A novel method for real-time atrial fibrillation detection in electrocardiograms using multiple parameters, Ann. Noninvasive Electrocardiol.: Off. J. Inter. Soc. Holter and Noninvasive Electrocardiology, Inc 19 (2014) 217–225.

[25] J. Lian, L. Wang, D. Muessig, A simple method to detect atrial fibrillation using RR intervals, Am. J. Cardiol. 107 (2011) 1494–1497.

[26] X. Zhou, H. Ding, B. Ung, E. Pickwell-MacPherson, Y. Zhang, Automatic online detection of atrial fibrillation based on symbolic dynamics and Shannon entropy, Biomed. Eng. Online 13 (2014) 18.

[27] A. Bardossy, A. Blinowska, W. Kuzmicz, J. Ollitrault, M. Lewandowski, A. Przybylski, Z. Jaworski, Fuzzy logic-based diagnostic algorithm for implantable cardioverter defibrillators, Artif. Intell. Med. 60 (2014) 113–121.

[28] O. Berenfeld, S. Ennis, E. Hwang, B. Hooven, K. Grzeda, S. Mironov, M. Yamazaki, J. Kalifa, J. Jalife, Time- and frequency-domain analyses of atrial fibrillation activation rate: the optical mapping reference, Heart Rhythm 8 (2011) 1758–1765.

[29] Z.C. Haberman, R.T. Jahn, R. Bose, H. Tun, J.S. Shinbane, R.N. Doshi, P.M. Chang, L.A. Saxon, Wireless smartphone ECG enables large-scale screening in diverse populations, J. Cardiovasc. Electrophysiol. 26 (2015) 520–526.

[30] L.S.B. Johnson, A.P. Persson, P. Wollmer, S. Juul-Möller, T. Juhlin, G. Engström, Irregularity and lack of p waves in short tachycardia episodes predict atrial fibrillation and ischemic stroke, Heart Rhythm 15 (2018) 805–811.

[31] R. Passman, Is a little atrial fibrillation still too much? Heart Rhythm 15 (2018) 812–813.

[32] R. Passman, J. Piccini, Electrocardiography screening for atrial fibrillation: we can do better, JAMA Cardiology (2018), https://doi.org/10.1001/jamacardio.2018.2200.

[33] O. Berenfeld, R. Mandapati, S. Dixit, A.C. Skanes, J. Chen, M. Mansour, J. Jalife, Spatially distributed dominant excitation frequencies reveal hidden organization in atrial fibrillation in the Langendorff-perfused sheep heart, J. Cardiovasc. Electrophysiol. 11 (2000) 869–879.

[34] T.H. Everett, E.E. Wilson, J.E. Olgin, Stable discrete high frequency sources as the mechanism of AF in dogs with heart failure, Heart Rhythm 1 (2004) S31.

[35] T.H.t. Everett, S. Verheule, E.E. Wilson, S. Foreman, J.E. Olgin, Left atrial dilatation resulting from chronic mitral regurgitation decreases spatiotemporal organization of atrial fibrillation in left atrium, Am. J. Physiol. Heart Circ. Physiol. 286 (2004) H2452–H2460.

[36] J. Kalifa, K. Tanaka, A.V. Zaitsev, M. Warren, R. Vaidyanathan, D. Auerbach, S. Pandit, K.L. Vikstrom, R. Ploutz-Snyder, A. Talkachou, F. Atienza, G. Guiraudon, J. Jalife, O. Berenfeld, Mechanisms of wave fractionation at boundaries of high-frequency excitation in the posterior left atrium of the isolated sheep heart during atrial fibrillation, Circulation 113 (2006) 626–633.

[37] P. Sanders, O. Berenfeld, M. Hocini, P. Jais, R. Vaidyanathan, L.F. Hsu, S. Garrigue, Y. Takahashi, M. Rotter, F. Sacher, C. Scavee, R. Ploutz-Snyder, J. Jalife, M. Haissaguerre, Spectral analysis identifies sites of high-frequency activity maintaining atrial fibrillation in humans, Circulation 112 (2005) 789–797.

[38] V.D. Corino, L.T. Mainardi, M. Stridh, L. Sornmo, Improved time–frequency analysis of atrial fibrillation signals using spectral modeling, IEEE Trans. Biomed. Eng. 55 (2008) 2723–2730.

[39] Y.P. Chen, D. Jeon, Y. Lee, Y. Kim, Z. Foo, I. Lee, N.B. Langhals, G. Kruger, H. Oral, O. Berenfeld, Z. Zhang, D. Blaauw, D. Sylvester, An injectable 64 nW ECG mixed-signal SoC in 65 nm for arrhythmia monitoring, IEEE J. Solid State Circ. 50 (2015) 375–390.

[40] R.G. Tieleman, Y. Plantinga, D. Rinkes, G.L. Bartels, J.L. Posma, R. Cator, C. Hofman, R.P. Houben, Validation and clinical use of a novel diagnostic device for screening of atrial fibrillation, Europace 16 (2014) 1291–1295.

[41] K.G. Tarakji, O.M. Wazni, T. Callahan, M. Kanj, A.H. Hakim, K. Wolski, B.L. Wilkoff, W. Saliba, B.D. Lindsay, Using a novel wireless system for monitoring patients after the atrial fibrillation ablation procedure: the iTransmit study, Heart Rhythm 12 (2015) 554–559.

[42] J. Park, S. Lee, M. Jeon, Atrial fibrillation detection by heart rate variability in Poincare plot, Biomed. Eng. Online 8 (2009) 38.

[43] X. Zhou, H. Ding, W. Wu, Y. Zhang, A real-time atrial fibrillation detection algorithm based on the instantaneous state of heart rate, PLoS One 10 (2015) e0136544.

[44] S.K. Sahoo, W. Lu, S.D. Teddy, D. Kim, M. Feng, Detection of Atrial fibrillation from non-episodic ECG data: a review of methods, Conference Proceedings : ... Annual International Conference of the IEEE Engineering in Medicine and Biology Society. IEEE Engineering in Medicine and Biology Society. Annual Conference, 2011, 2011, pp. 4992–4995.

[45] B. Freedman, J. Camm, H. Calkins, J.S. Healey, M. Rosenqvist, J. Wang, C.M. Albert, C.S. Anderson, S. Antoniou, E.J. Benjamin, G. Boriani, J. Brachmann, A. Brandes, T.F. Chao, D. Conen, J. Engdahl, L. Fauchier, D.A. Fitzmaurice, L. Friberg, B.J. Gersh, D.J. Gladstone, T.V. Glotzer, K. Gwynne, G.J. Hankey, J. Harbison, G.S. Hillis, M.T. Hills, H. Kamel, P. Kirchhof, P.R. Kowey, D. Krieger, V.W.Y. Lee, L.A. Levin, G.Y.H. Lip, T. Lobban, N. Lowres, G.H. Mairesse, C. Martinez, L. Neubeck, J. Orchard, J.P. Piccini, K. Poppe, T.S. Potpara, H. Puererfellner, M. Rienstra, R.K. Sandhu, R.B. Schnabel, C.W. Siu, S. Steinhubl, J.H. Svendsen, E. Svennberg, S. Themistoclakis, R.G. Tieleman, M.P. Turakhia, A. Tveit, S.B. Uittenbogaart, I.C. Van Gelder, A. Verma, R. Wachter, B.P. Yan, Screening for atrial fibrillation: a report of the AF-SCREEN international collaboration, Circulation 135 (2017) 1851–1867 doi: 1810.1161/CIRCULATIONAHA.1116.026693.

[46] M. Lown, J. Garrard, G. Irving, D. Edwards, F.R. Hobbs, J. Mant, Should we screen for atrial fibrillation? Br. J. Gen. Pract. 67 (2017) 296–297.

[47] G.H. Mairesse, P. Moran, I.C. Van Gelder, C. Elsner, M. Rosenqvist, J. Mant, A. Banerjee, B. Gorenek, J. Brachmann, N. Varma, G. Glotz de Lima, J. Kalman, N. Claes, T. Lobban, D. Lane, G.Y.H. Lip, G. BorianiE.S.C.S.D. Group, Screening for atrial fibrillation: a european heart rhythm association (EHRA) consensus document endorsed by the heart rhythm society (HRS), Asia Pacific heart rhythm society (APHRS), and Sociedad Latinoamericana de Estimulación Cardíaca y Electrofisiología (SOLAECE), EP Europace 19 (2017) 1589–1623.

[48] S.Y. Shin, G.Y.H. Lip, The importance and future of population screening for atrial fibrillation, Can. J. Cardiol. 34 (2018).

[49] A.E. Darby, Recurrent atrial fibrillation after catheter ablation: considerations for repeat ablation and strategies to optimize success, J. Atr. Fibrillation 9 (2016) 1427.

[50] C.W. Israel, G. Grönefeld, J.R. Ehrlich, Y.-G. Li, S.H. Hohnloser, Long-term risk of recurrent atrial fibrillation as documented by an implantable monitoring device, Implications for optimal patient care 43 (2004) 47–52.

[51] O.A. Ajijola, N.G. Boyle, K. Shivkumar, Detecting and monitoring arrhythmia recurrence following catheter ablation of atrial fibrillation, Front. Physiol. 6 (2015).

[52] D.A. Whalen, P.M. Covelle, J.C. Piepenbrink, K.L. Villanova, C.L. Cuneo, E.H. Awtry, Novel approach to cardiac alarm management on telemetry units, J. Cardiovasc. Nurs. 29 (2014) E13–E22.

[53] M. Hravnak, T. Pellathy, L. Chen, A. Dubrawski, A. Wertz, G. Clermont, M.R. Pinsky, A call to alarms: current state and future directions in the battle against alarm fatigue, J. Electrocardiol. 51 (2018).

[54] I.C. Van Gelder, M.E.W. Hemels, The progressive nature of atrial fibrillation: a rationale for early restoration and maintenance of sinus rhythm, EP Europace 8 (2006) 943–949.

[55] M. Van Zyl, C. McLeod, B. Gersh, Approach to device-detected subclinical atrial fibrillation, SA Heart (2017) 14.